

High-Resolution Fourier Transform Spectrum of HDO in the Region 6140–7040 cm⁻¹

O. N. Ulenikov,* Shui-Ming Hu,† E. S. Bekhtereva,* G. A. Onopenko,* Xiang-Huai Wang,†
Sheng-Gui He,† Jing-Jing Zheng† and Qing-Shi Zhu†

*Laboratory of Molecular Spectroscopy, Physics Department, Tomsk State University, Tomsk, 634050, Russia; and †Open Research
Laboratory of Bond-Selective Chemistry, University of Science and Technology of China, Hefei, 230026, P.R. China

E-mail: Ulenikov@phys.tsu.ru; smhu@ustc.edu.cn

Received March 25, 2001; in revised form May 23, 2001; published online July 31, 2001

The high-resolution Fourier transform spectrum of the HDO molecule was recorded and analyzed in the region 6140–7040 cm⁻¹ where the bands $\nu_1 + \nu_3$, $2\nu_2 + \nu_3$, and $2\nu_1 + \nu_2$ are located. The presence of strong local resonance interactions allowed us to assign some tens of transitions to the weak bands $5\nu_2$ and $\nu_1 + 3\nu_2$ as well. Spectroscopic parameters of the analyzed bands were estimated. They reproduce initial upper energies with the accuracy close to experimental uncertainties. © 2001 Academic Press

Key Words: vibration–rotation spectra; HDO molecule; spectroscopic parameters.

1. INTRODUCTION

In the present contribution, we continue our spectroscopic study of the deuterated species of the H₂O molecule (*I–5*) in a shortwave region. In this case, the spectrum of HDO in the region 6140–7040 cm⁻¹ was recorded with the Bruker IFS 120HR Fourier-transform interferometer (Hefei, China).

Because a detailed review of earlier contributions concerning the high-resolution spectroscopic studies of the HDO molecule has been presented in our recent paper (3), we omit it here and mention only (a) the papers by A. Campargue and his co-authors (6–8), which were devoted to the rotational analysis of highly excited vibrational states of the HDO molecule and published in 2000, and (b) excellent *ab initio* predictions of the rovibrational energies carried out by Partridge and Schwenke (9). As to the region near 1.4 μm studied in this work, it was first analyzed using a grating spectrometer with a medium resolution of about 0.2 cm⁻¹ by Benedict *et al.* (10), where transitions belonging to the $\nu_1 + \nu_3$ and $2\nu_2 + \nu_3$ bands were recorded and upper energies were derived up to $J^{\text{max.}} = 12$ and 9 for the vibrational states (101) and (021), respectively.

Next the HDO spectrum in the mentioned region was studied by Ohshima and Sasada (11), who recorded the absorption spectrum of the same $\nu_1 + \nu_3$ and $2\nu_2 + \nu_3$ bands using a single-mode distributed feedback semiconductor laser which provided a considerably better experimental accuracy of about 0.004 cm⁻¹. In that case, the upper energies were derived up to $J^{\text{max.}} = 13$ and 11 for the states (101) and (021), respectively. Ohshima and Sasada derived the spectroscopic parameters which reproduced the assigned 537 HDO lines with the following accuracy: 68.3% of the lines were reproduced with accuracy $0 \leq \delta < 4 \times$

10^{-3} cm⁻¹, 26.1% with accuracy $4 \leq \delta < 8 \times 10^{-3}$ cm⁻¹, and 5.6% with accuracy $8 \leq \delta < 15 \times 10^{-3}$ cm⁻¹.

In 1997, Toth measured the HDO spectrum in the region 6000–7700 cm⁻¹ with high resolution of 0.012–0.020 cm⁻¹ (12). The 2445 transitions were assigned to the $\nu_1 + \nu_3$, $2\nu_2 + \nu_3$, $2\nu_1 + \nu_2$, and $2\nu_3$ bands of the HDO species. On that basis, upper energies of the (101), (021), (210), and (002) vibrational states up to $J^{\text{max.}} = 15, 13, 12,$ and 19, respectively, were determined, but the least squares fit analysis was absent in (12).

In this paper, we present the results of new analysis of the high-resolution Fourier transform spectrum of the HDO molecule in the region 6140–7040 cm⁻¹ where the bands $\nu_1 + \nu_3$, $2\nu_2 + \nu_3$, and $2\nu_1 + \nu_2$ are located. Experimental details are discussed in Section 2. Section 3 is devoted to description of the Hamiltonian model used in the fit of experimental data. The results of assignment and discussion are presented in Section 4.

2. EXPERIMENTAL DETAILS

The sample of D₂¹⁶O was purchased from PeKing Chemical Industry, Ltd. (China). The stated purity of deuterium was 99.8%. The spectra were recorded at room temperature with the Bruker IFS 120HR Fourier-transform interferometer (Hefei, China), which is equipped with a path length adjustable multipass gas cell, a tungsten source, a CaF₂ beamsplitter, and Ge diode detector. The unapodized resolution was 0.01 cm⁻¹, and the apodization function was Blackman–Harris 3-Term.

Since in the region under study there are many lines due to the absorption of H₂O and D₂O, two spectra were measured with different ratios of HDO to D₂O and H₂O. The first spectrum was recorded at a total pressure of 1516 Pa with the percentage

of HDO being approximately 44% and the path length being 87 m. The corresponding conditions of the second spectrum were 1500 Pa, 15% and 69 m, respectively. The line positions of such lines saturated in the first spectrum were picked out from the second spectrum while others were picked out from the first one. All the line positions were calibrated with those of the H₂O from the GEISA97 database. The accuracy of the unblended lines was estimated to be 0.0007 cm⁻¹. For illustration, two small pieces of the recorded spectra are presented in Fig. 1 and Fig. 2.

3. HAMILTONIAN MODEL

As was mentioned in the Introduction, the absorption spectrum of the HDO molecule in the region of 6140–7040 cm⁻¹ is caused by three bands $\nu_1 + \nu_3$, $2\nu_2 + \nu_3$, and $2\nu_1 + \nu_2$ with the band centers near 6415, 6452, and 6745 cm⁻¹, respectively (data from Ref. (13)). Moreover, as can be seen from the same reference (13), two additional weak bands, $5\nu_2$ and $\nu_1 + 3\nu_2$, with the band centers near 6688 and 6851 cm⁻¹, respectively, are located close to the three mentioned vibrational bands. For this reason, the theoretical analysis of the spectrum and the fit of experimental data were based on the following form of the effective rotational Hamiltonian:

$$H^{eff.} = \sum_{v,v'} |v\rangle \langle v'| H^{vv'}. \quad [1]$$

This Hamiltonian takes into account resonance interactions between all the five vibrational states (101), (021), (210), (130), and (050). Here the following notations are used: |1⟩ = (101), |2⟩ = (021), |3⟩ = (210), |4⟩ = (130), and |5⟩ = (050). The diagonal operators H^{vv} ($v = 1, 2, 3, 4, 5$) are the usual Watson's rotational operators, Ref. (14):

$$\begin{aligned} H^{vv} = & E^v + \left[A^v - \frac{1}{2}(B^v + C^v) \right] J_z^2 + \frac{1}{2}(B^v + C^v) J^2 \\ & + \frac{1}{2}(B^v - C^v) J_{xy}^2 - \Delta_K^v J_z^4 - \Delta_{JK}^v J_z^2 J^2 \\ & - \Delta_J^v J^4 - \delta_K^v [J_z^2, J_{xy}^2]_+ - 2\delta_J^v J^2 J_{xy}^2 + H_K^v J_z^6 \\ & + H_{KJ}^v J_z^4 J^2 + H_{JK}^v J_z^2 J^4 + H_J^v J^6 + [J_{xy}^2, h_K^v J_z^4] \\ & + h_{JK}^v J^2 J_z^2 + h_J^v J^4]_+ + L_K^v J_z^8 + L_{KKJ}^v J_z^6 J^2 \\ & + L_{KJ}^v J_z^4 J^4 + L_{KJJ}^v J_z^2 J^6 + L_J^v J^8 + [J_{xy}^2, l_K^v J_z^6 \\ & + l_{KJ}^v J^4 J_z^2 + l_{JK}^v J^2 J_z^4 + l_J^v J^6]_+ + P_K^v J_z^{10} + \dots \quad [2] \end{aligned}$$

Operators $H^{vv'}$ ($v \neq v'$) account for the operators of resonance interactions. Since HDO is a prolate asymmetric top molecule the symmetry of which is isomorphic to the C_i symmetry group, any of its three vibrational coordinates is transformed according to the totally symmetric irreducible representation of the C_i group. As a consequence, all resonance interaction blocks

have the similar form and should be written as a sum of two terms,

$$H^{vv'} = H^{vv'+} = H_{F.}^{vv'} + H_{C.}^{vv'}, \quad [3]$$

which describe resonance interactions of the Fermi type and Coriolis type respectively:

$$\begin{aligned} H_{F.}^{vv'} = & F_0^{vv'} + F_K^{vv'} J_z^2 + F_J^{vv'} J^2 + F_{KK}^{vv'} J_z^4 + F_{KJ}^{vv'} J_z^2 J^2 \\ & + F_{JJ}^{vv'} J^4 + \dots + F_{xy}^{vv'} J_{xy}^2 + F_{xyK}^{vv'} [J_{xy}^2, J_z^2]_+ \\ & + F_{xyJ}^{vv'} J_{xy}^2 J^2 + \dots \quad [4] \end{aligned}$$

$$\begin{aligned} H_{C.}^{vv'} = & C_y^{vv'} i J_y + C_{yK}^{vv'} [i J_y, J_z^2]_+ + C_{yJ}^{vv'} i J_y J^2 \\ & + C_{yKK}^{vv'} [i J_y, J_z^4]_+ + C_{yKJ}^{vv'} [i J_y, J_z^2]_+ J^2 + C_{yJJ}^{vv'} i J_y J^4 \\ & + \dots + C_{xz}^{vv'} [J_x, J_z]_+ + C_{xzK}^{vv'} [[J_x, J_z]_+, J_z^2]_+ \\ & + C_{xzJ}^{vv'} [J_x, J_z]_+ J^2 + \dots \quad [5] \end{aligned}$$

In Eqs. [2]–[5] the following notations are used: $J_{xy}^2 = J_x^2 - J_y^2$, $J^2 = \sum_{\alpha} J_{\alpha}^2$, and $[A, B]_+ = AB + BA$.

4. ASSIGNMENT OF TRANSITIONS AND DISCUSSION

Since HDO is a prolate asymmetric top molecule and its symmetry group is isomorphic C_i type symmetry, any of its vibrational–rotational bands contains absorption lines arising from transitions of two types (both A and B). In this case, comparison of the transitions of both types in these three bands, $\nu_1 + \nu_3$, $2\nu_2 + \nu_3$, and $2\nu_1 + \nu_2$, shows that the B -type transitions in the $\nu_1 + \nu_3$ band are the strongest. As an illustration, Table 1 presents line strengths of the “pilot” transitions [$J = 5K'_a K'_c = 5$] \leftarrow [$J = 6K_a K_c = 6$] ($K'_a, K_a = 0$ and/or 1) for all the three mentioned bands. From Table 1 one can see that

TABLE 1
List of the “Pilot” Transitions in the $\nu_1 + \nu_3$, $2\nu_2 + \nu_3$, and $2\nu_1 + \nu_2$ Absorption Bands of the HDO Molecule

Band	Upper J'	K'_z	K'_c	Lower J	K_a	K_c	Line position, in cm ⁻¹	Intensity ^{a)}	Relative intensity
1	2	3	4	5	6				
(101)	5	0	5	6	0	6	6325.5901	4.4	0.5
(101)	5	0	5	6	1	6	6323.2899	20.5	2.0
(101)	5	1	5	6	0	6	6329.1380	19.1	2.0
(101)	5	1	5	6	1	6	6328.8366	4.0	0.5
(021)	5	0	5	6	0	6	6365.5914	7.8	1.0
(021)	5	0	5	6	1	6	-	-	-
(021)	5	1	5	6	0	6	6370.2720	0.1	0.02
(021)	5	1	5	6	1	6	6367.9738	7.6	1.0
(210)	5	0	5	6	0	6	6655.6639	7.7	1.0
(210)	5	0	5	6	1	6	6653.3630	1.7	0.2-0.25
(210)	5	1	5	6	0	6	6661.6640	1.7	0.2-0.25
(210)	5	1	5	6	1	6	6659.3625	6.9	1.0

^a In 10⁻²³ cm⁻¹/(molecule cm⁻²).

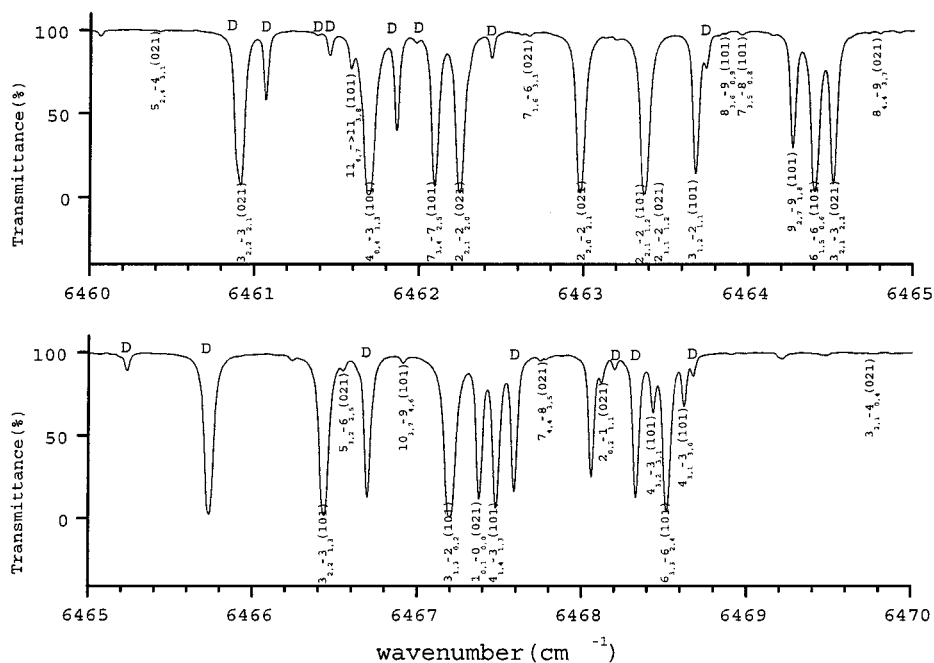


FIG. 1. Part of the spectrum: transitions in the region 6460–6470 cm^{-1} . Assignments of HDO are given; lines marked by “D” belong to D_2O . See text for experimental details.

the *A*-type transitions in the $\nu_1 + \nu_3$ band are roughly four times weaker than the *B*-type ones; strengths of the *A*-type transitions in the $2\nu_2 + \nu_3$ and $2\nu_1 + \nu_2$ bands are comparable and roughly two times weaker than those of the *B*-type transitions in the

$\nu_1 + \nu_3$ band. In turn, the *B*-type transitions in the $2\nu_2 + \nu_3$ and $2\nu_1 + \nu_2$ bands are very weak (see Table 1 for details).

The recorded transitions were assigned using the ground state combination differences method, and the ground state rotational

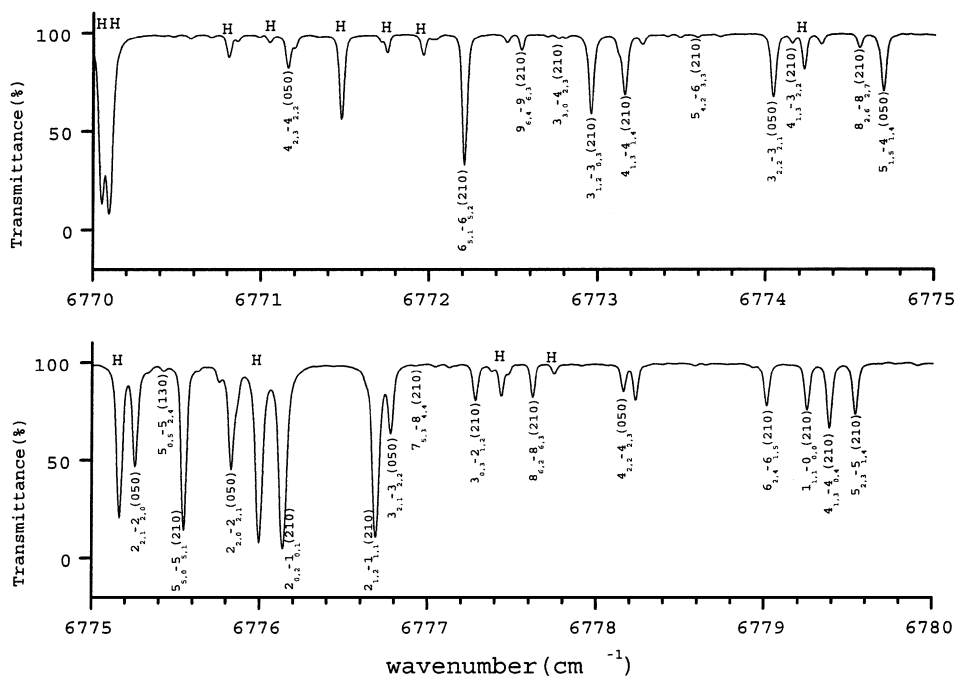


FIG. 2. Part of the spectrum: transitions in the region 6770–6780 cm^{-1} . Assignments of HDO are given; lines marked by “H” belong to H_2O . See text for experimental details.

TABLE 2
 Experimental Rovibrational Term Values for the (101), (210), and (021) Vibrational States of the HDO Molecule (in cm^{-1})^a

J	K _a	K _c	(101)			(210)			(021)		
			E	Δ	δ	E	Δ	δ	E	Δ	δ
			1	2	3	4	5	6	7	8	9
0	0	0	6415.4601	5	4	6746.9081	4	5	6451.8996	8	4
1	0	1	6430.6574	1	-4	6761.9314	4	1	6467.3743	7	-5
1	1	1	6444.6100	6	2	6779.2502	4	6	6484.0424	6	4
1	1	0	6447.3760	1	2	6782.1016	6	3	6487.1479	8	1
2	0	2	6460.6689	8	0	6791.6433	3	0	6497.9266	11	-2
2	1	2	6472.2047	5	2	6806.4983	5	5	6511.8994	4	5
2	1	1	6480.4887	2	1	6815.0578	3	2	6521.1294	10	17
2	2	1	6521.4969	2	-2	6855.4604	4	8	6571.5118	3	7
2	2	0	6521.7805	6	-6	6855.7873	4	5	6571.9046	2	6
3	0	3	6504.7701	6	-4	6835.4069	2	0	6542.8002	8	-7
3	1	3	6513.3673	2	0	6847.1735	4	3	6553.4440	3	-2
3	1	2	6529.8643	5	-2	6864.2882	4	0	6572.0544	1	7
3	2	2	6566.8212	5	2	6900.5621	3	-5	6617.9802	4	2
3	2	1	6568.6402	4	0	6902.1692	3	-4	6619.9002	3	2
3	3	1	6640.3893	6	2	6989.7784	4	0	6709.5719	4	-16
3	3	0	6640.4204	5	-2	6989.8028	10	-3	6709.6025	20	-21
4	0	4	6562.0870	5	-5	6892.4220	4	0	6601.0618	7	-4
4	1	4	6567.8658	3	0	6901.0732	5	-3	6608.4299	4	-6
4	1	3	6595.1136	4	-4	6929.5400	6	-7	6639.2520	2	1
4	2	3	6627.0687	4	2	6960.3826	6	-5	6679.6024	4	0
4	2	2	6632.2107	5	1	6965.0149	3	-9	6685.0981	3	2
4	3	2	6701.4548	3	-1	7050.0920	1	0	6772.1942	2	-4
4	3	1	6701.6716	5	-2	7050.2639	2	-2	6772.4095	4	-3
4	4	1	6801.6468	2	1	7168.0798	7	-6	6897.6751	79	-6
4	4	0	6801.6492	11	2	7168.0810		-9	6897.6751	79	-59
5	0	5	6631.9050	4	-3	6961.9785	2	2	6671.9059	13	-7
5	1	5	6635.4525	6	-2	6967.9783	3	-7	6676.5896	7	-5
5	1	4	6675.6593	5	-4	7010.4894	6	-11	6722.2542	3	5
5	2	4	6701.8668	6	0	7034.6639	7	-6	6756.0970	11	-14
5	2	3	6712.8708	7	1	7044.7733	5	-1	6767.9790	2	1
5	3	3	6777.8908	4	-1	7125.5935	8	7	6850.5861	2	-3
5	3	2	6778.7338	5	-1	7126.3420	2	-1	6851.4251	2	1
5	4	2	6877.7813	3	-2	7243.2524	12	12	6975.8255	6	5
5	4	1	6877.8011	2	-3	7243.2631	19	-15	6975.8434	7	-7
5	5	1	7004.5780	9	9	7391.5155	5	-3	7133.5702	10	-1
5	5	0	7004.5780	9	7	7391.5155	5	-4	7133.5702	10	-3
6	0	6	6713.8688	7	0	7043.6604	5	7	6754.8888	3	3
6	1	6	6715.8991	5	-1	7047.6816	4	-11	6757.6726	20	17
6	1	5	6770.7144	3	-3	7106.8288	7	-7	6820.2594	2	2
6	2	5	6790.8995	3	-3	7123.1060	5	0	6847.1330	1	-1
6	2	4	6810.5546	6	7	7141.5197	9	10	6868.4178	7	-3
6	3	4	6869.7932	7	1	7216.2512	6	7	6944.6961	1	0
6	3	3	6872.0635	6	2	7218.1644	5	1	6947.1163	5	9
6	4	3	6969.3104	3	-4	7333.6093	6	6	7069.7723	7	4
6	4	2	6969.4078	4	-1	7333.6750	8	-2	7069.8620	19	-10
6	5	2	7095.6185	30	17	7481.3735	25	10	7227.0721	35	10
6	5	1	7095.6185	30	2	7481.3743	25	9	7227.0721	35	-3
6	6	1	7248.3084	20	-18	7658.8890	4	6	7414.7709	10	3
6	6	0	7248.3084	20	-18	7658.8890	4	6	7414.7709	10	4
7	0	7	6807.9106	5	0	7137.3392	12	21	6849.8874	5	7
7	1	7	6809.0158	4	-2	7140.0083	5	-16	6851.4605	2	-2
7	1	6	6879.3347	4	1	7218.4852	9	7	6932.2794	3	-1
7	2	6	6893.8178	4	-2	7225.3864	7	1	6952.3365	2	-13
7	2	5	6924.8032	5	5	7255.0084	4	-7	6986.5451	15	-14
7	3	5	6976.4673	3	-2	7321.9587	10	2	7054.3763	5	-2
7	3	4	6982.2146	4	0	7326.5214	10	-1	7060.0676	10	4
7	4	4	7076.2883	4	-8	7439.2086	5	4	7179.5707	5	4
7	4	3	7076.6345	9	-2	7439.4469	6	-1	7179.8919	2	0
7	5	3	7201.9576	8	2	7586.3224	49	17	7336.2720	30	-5
7	5	2	7201.9670	11	1	7586.3288	5	27			

^a Δ is the experimental uncertainty of the energy value, equal to one standard deviation in units of 10^{-4} cm^{-1} ; δ is the difference $E^{\text{exp.}} - E^{\text{calc.}}$, also in units of 10^{-4} cm^{-1} ; Δ is not quoted when the energy value was obtained from only one transition.

TABLE 2—Continued

<i>J</i>	<i>K_a</i>	<i>K_c</i>	(101)			(210)			(021)		
			<i>E</i>	Δ	δ	<i>E</i>	Δ	δ	<i>E</i>	Δ	δ
	1		2	3	4	5	6	7	8	9	10
7	6	2	7354.1114	8	6	7763.2669	8	7	7523.4695	13	-6
7	6	1	7354.1114	8	5	7763.2669	8	7	7523.4695	13	-1
7	7	1	7531.8100	6	1	7967.8802	11	-14	7738.8709	9	4
7	7	0	7531.8100	6	1	7967.8802	11	-14	7738.8709	9	4
8	0	8	6914.0786	2	1	7243.0343	11	6	6956.9365	2	15
8	1	8	6914.6595	3	-2	7244.8281	6	-8	6957.7959	3	5
8	1	7	7000.6000	9	1	7345.7870	7	4	7057.2902	1	-3
8	2	7	7010.2625	3	-1	7341.0487	4	6	7071.3224	11	-1
8	2	6	7054.9112	5	4	7384.4960	8	0	7121.0423	1	-1
8	3	6	7098.2837	6	-1	7442.5297	1	15	7179.3727	7	6
8	3	5	7109.6562	8	4	7451.8136	3	-14	7190.8205	3	-6
8	4	5	7198.7494	14	4	7560.0798	3	-6	7305.2382	10	2
8	4	4	7199.7320	13	24	7560.7771	4	-2	7306.1611	3	-17
8	5	4	7323.6505	4	-5	7706.3400	28	19	7461.2106		-69
8	5	3	7323.6907	5	-22	7706.4213	17	8			
8	6	3	7475.1098	9	20	7882.6231	2	-5	7647.7514	11	-24
8	6	2	7475.1098	9	11	7882.6231	2	-8	7647.7514	11	.26
8	7	2	7652.2105	3	-1				7862.5884	14	3
8	7	1	7652.2105	3	-1				7862.5884	14	3
8	8	1	7853.8729		0						
8	8	0	7853.8729		0						
9	0	9	7032.4289	2	2	7360.8155	3	5	7076.0984	5	20
9	1	9	7032.7269	2	1	7362.0522	6	0	7076.5570	2	13
9	1	8	7133.8598	10	0	7457.9025	5	4	7194.4769	3	2
9	2	8	7139.8926	4	-1	7469.9644	3	-22	7203.7125	3	-6
9	2	7	7200.0006	6	6	7529.3089	6	1	7271.2296	1	0
9	3	7	7234.6839	5	-3	7577.6660	6	3	7319.2282	2	13
9	3	6	7254.5194	7	2	7594.3527	2	3	7339.8862	2	15
9	4	6	7336.4121	9	-13	7696.2085	5	1	7446.7322	11	5
9	4	5	7339.0666	18	-47	7697.9623	3	2	7449.0124		-45
9	5	5	7460.7487	7	-13	7841.6465	7	4			
9	5	4	7460.8805	18	24	7841.7259	18	28			
9	6	4	7611.3352	4	5	8016.9804	48	27			
9	6	3	7611.3374	11	-18	8016.9804	48	11			
10	0	10	7162.9933	7	1	7490.7316	17	-37	7207.4123	10	1
10	1	10	7163.1435	5	0	7491.6580	44	5	7207.6541	12	-23
10	1	9	7278.8400	5	0	7604.3403	10	1	7343.3963	1	4
10	2	9	7282.4071	5	-3	7611.6891		48	7349.1720	1	6
10	2	8	7359.0587	5	3	7688.5093	4	-7	7435.9772	4	-16
10	3	8	7385.2978	3	0	7727.0953	7	-1	7474.2146	10	2
10	3	7	7416.4853	5	2	7754.0096	8	5	7506.5760	6	-3
10	4	7	7489.6600	7	6	7847.5194	2	-1	7603.9089	3	2
10	4	6	7495.1204	4	1	7851.1366	4	4	7608.8162	2	1
10	5	6	7613.3410	5	-38				7758.4399	11	-2
10	5	5	7613.6694	8	1						
11	0	11	7305.7799	3	3	7632.8683	8	-5	7350.9123	5	13
11	1	11	7305.8543	3	-1	7633.2211	13	-5	7351.0367	2	6
11	1	10	7435.5359	4	-3				7503.9430	3	2
11	2	10	7437.5602	4	2				7507.4147	4	8
11	2	9	7531.0320	8	3						
11	3	9	7549.7200	10	8	7890.4093	6	-2	7643.2737	2	-1
11	3	8	7594.8617	10	-3	7930.5873	3	1	7690.6478	9	9
11	4	8	7657.8662	6	-51						
11	4	7	7668.3377	7	-10						
11	5	7	7781.0498	1	-4						
12	0	12	7460.7777	3	4	7786.9004	9	0	7506.5823	13	2
12	1	12	7460.8142	4	0				7506.6475	9	11
12	1	11	7604.0470	5	3				7676.1916	13	3
12	2	11	7605.1600	17	1						
12	2	10	7715.0097	10	-26						
12	3	10	7727.5432	15	8						
12	4	9	7840.8458	15	-24						
12	4	8	7859.0488	8	19						
12	5	8	7964.4446	30	0						

TABLE 2—Continued

<i>J</i>	<i>K_a</i>	<i>K_c</i>	(101)			(210)			(021)		
			<i>E</i>	Δ	δ	<i>E</i>	Δ	δ	<i>E</i>	Δ	δ
			1	2	3	4	5	6	7	8	9
13	0	13	7627.9654	4	12	7953.4753	20	-12	7674.4153	2	20
13	1	13	7627.9800	21	-22				7674.4442	6	-20
13	1	12	7784.4684	9	15				7860.2569	2	-6
13	2	12	7785.0674	10	23				7861.4166	17	4
13	2	11	7910.4267	20	-9						
13	3	11	7918.3842	13	17						
13	4	10	8038.2132	10	17						
14	0	14	7807.3104	28	3				7854.3810	5	17
14	1	14	7807.3194	23	5						
14	1	13	7976.8520	3	-31						
14	2	13	7977.1706	5	-4						
15	0	15	7998.7830	30	-6				8046.4570	84	98
15	1	15	7998.7830	30	37				8046.4570	84	13
15	1	14	8181.2326	13	-9						
15	2	14	8181.4006	3	26						
16	0	16	8202.3319	11	5						
16	1	16	8202.3319	11	-15						

energies were calculated on the basis of the parameters from Ref. (15). As a result of the analysis, we assigned undoubtedly 888 transitions with $J^{max.} = 16$ and $K_a^{max.} = 8$ to the $\nu_1 + \nu_3$ band, 562 transitions with $J^{max.} = 15$ and $K_a^{max.} = 7$ to the $2\nu_2 + \nu_3$ band, and 503 transitions with $J^{max.} = 13$ and $K_a^{max.} = 7$ to the $2\nu_1 + \nu_2$ one. Two small parts of the recorded spectrum with the assigned transitions are shown in Fig. 1 and Fig. 2. Upper energies belonging to the (101), (021), and (210) vibrational states were obtained from the assigned transitions. They are presented in columns 2, 5, and 8 of Table 2, respectively. The values of Δ in columns 3, 6, and 9 indicate the experimental uncertainties of the energy levels equal to one standard deviation in units of 10^{-4} cm^{-1} .

It should be noted that the experimental transitions were assigned simultaneously with the fitting of the obtained upper energies on the basis of the Hamiltonian [1]–[5]. We believe that just this allowed us to obtain the following results:

(1) *Some tens of transitions were assigned to the weak bands $5\nu_2$ and $\nu_1 + 3\nu_2$.* As was mentioned above, strong resonance interactions occur not only inside the “bright” states (101), (021), and (210), but also between the “bright” states and the “dark” ones, (130) and (050). As a consequence, transitions caused by such resonance interactions and belonging to the $5\nu_2$ and $\nu_1 + 3\nu_2$ can appear in the recorded spectrum. However, such transitions are very weak, as a rule, and the problem of their undoubted assignment in the spectrum is not trivial. In this situation, fitting of the experimental energies belonging to the (101), (021), and (210) vibrational states and strongly perturbed by the resonance interactions with the (050) and (130) states gives a good basis for correct prediction of the upper energies belonging to the (050) and (130) states. As a result, we suc-

ceeded in assignment of some tens of transitions to the $5\nu_2$ and $\nu_1 + 3\nu_2$ bands. Lists of transitions undoubtedly assigned to the $5\nu_2$ and $\nu_1 + 3\nu_2$ bands are presented in columns 3 of Table 3 and Table 4, respectively. Columns 4 of these tables show corresponding transmittancy of transitions in percent. Columns 5 and 6 give the values of upper energies obtained from the corresponding transitions and their mean values. Some transitions assigned to the $5\nu_2$ and $\nu_1 + 3\nu_2$ bands can be seen in Fig. 2.

(2) Results of our analysis demonstrate good correlation with the earlier results by Toth (12). However, the results of the fit show that *some transitions with high values of the quantum number J belonging to the $2\nu_2 + \nu_3$, and $2\nu_1 + \nu_2$ bands were misassigned in (12).* As an illustration, the upper energies $E_{[551](021)}^{exp.} = 7133.5702 \pm 0.0010 \text{ cm}^{-1}$, $E_{[651](021)}^{exp.} = 7227.0721 \pm 0.0035 \text{ cm}^{-1}$, $E_{[770](210)}^{exp.} = 7967.8802 \pm 0.0011 \text{ cm}^{-1}$ can be mentioned. It should be noted that these values correlate very well with those calculated with the parameters determined from the fit (7133.5703, 7227.0724, and 7967.8816 cm^{-1} , respectively). At the same time, the corresponding values determined in Ref. (12) (7124.0057, 7218.2197, and 7972.0404 cm^{-1} , respectively) differ widely from the calculated ones.

It should be also noted that our upper energies presented in Table 2 differ a little from the corresponding energies of Ref. (12). This can be explained by three reasons:

(a) Different literature sources were used for calibration of experimental data.

(b) As was mentioned in Section 2, we estimate the accuracy of our experimental line positions as 0.0007 cm^{-1} (the comparison of our line positions with those presented in Table 2 of Ref. (12) shows, as a rule, just such differences in line positions).

TABLE 3
List of Transitions Belonging to the $5\nu_2$ Band of HDO

J'	Upper K'_a	K'_c	J	Lower K_a	K_c	Line position, in cm^{-1}	Transmit., in per cent	Upper energy, in cm^{-1}	Mean value, in cm^{-1}	δ in 10^{-4} cm^{-1}
	1			2		3	4	5	6	7
1	1	1	1	1	0	6707.5754	85.6	6740.0717	6740.0722	17
			2	1	2	6681.9459	85.2	6740.0728		
1	1	0	1	1	1	6713.8350	85.4	6743.6435	6743.6439	8
			1	0	1	6728.1353	98.1	6743.6435		
			2	1	1	6677.4596	87.7	6743.6441		
			2	2	1	6634.7186	98.3	6743.6448		
2	1	1	1	1	0	6745.8213	83.7	6778.3176	6778.3176	-7
			2	1	2	6720.1909	91.1	6778.3178		
			3	1	2	6661.8567	81.0	6778.3179		
			2	0	2	6732.1443	97.5	6778.3174		
2	0	2	1	0	1	6721.4270	90.7	6736.9352	6736.9352	-1
			2	1	1	6670.7531	98.6	6736.9376		
2	1	2	1	1	1	6737.8195	84.5	6767.6281	6767.6280	0
			2	1	1	6701.4435	92.7	6767.6281		
			1	0	1	6752.1197	97.3	6767.6279		
2	2	0	1	1	1	6854.9455	90.0	6884.7541	6884.7540	-1
			2	1	1	6818.5695	93.7	6884.7541		
			2	2	1	6775.8281	45.1	6884.7543		
			3	2	1	6727.6889	73.9	6884.7536		
2	2	1	2	1	2	6826.3980	93.3	6884.5250	6884.5251	-17
			2	2	0	6775.2560	46.5	6884.5251		
			3	1	2	6768.0640	97.6	6884.5252		
3	2	2	2	1	1	6864.9201	91.9	6931.1046	6931.1046	-1
			2	2	1	6822.1781	69.1	6931.1043		
			3	2	1	6774.0403	67.1	6931.1050		
			4	2	3	6714.0621	68.9	6931.1039		
			3	3	1	6698.0816	97.4	6931.1052		
3	2	1	2	1	2	6874.0410	91.1	6932.1680	6932.1680	-17
			4	2	2	6710.3323	70.5	6932.1681		
			3	1	2	6815.7068	92.9	6932.1681		
			3	3	0	6699.1169	97.3	6932.1680		
			4	3	2	6636.6808	94.1	6932.1679		
3	1	2	3	1	3	6729.6719	93.3	6830.0628	6830.0620	1
			3	0	3	6738.7329	96.0	6830.0631		
			4	1	3	6647.0778	76.4	6830.0612		
			4	2	3	6613.0191	96.7	6830.0610		
3	1	3	2	1	2	6750.6520	44.4	6808.7789	6808.7812	-26
			2	0	2	6762.6105	97.7	6808.7835		
			4	1	4	6652.3999	79.0	6808.7821		
3	0	3	2	0	2	6736.4400	88.8	6782.6131	6782.6131	-7
			4	0	4	6632.4568	88.6	6782.6130		
4	1	3	3	2	2	6743.1246	98.5	6898.5136	6898.5148	10
			4	0	4	6748.3576	94.9	6898.5137		
			5	1	4	6633.2802	70.2	6898.5161		
4	2	2	3	1	3	6894.8106	88.2	6995.2015	6995.2015	1
			3	2	1	6838.1365	71.6	6995.2012		
			4	2	3	6778.1591	84.9	6995.2009		
			5	2	3	6691.2075	79.4	6995.2022		
4	2	3	4	1	4	6836.6099	92.8	6992.9921	6992.9919	1
			3	2	2	6837.6023	61.0	6992.9913		
			4	2	2	6771.1563	81.9	6992.9923		
			5	2	4	6699.3560	70.7	6992.9925		
5	0	5	4	0	4	6764.8940	83.6	6915.0501	6915.0498	4
			6	0	6	6608.7350	86.2	6915.0495		
5	1	5	4	1	4	6774.6957	70.1	6931.0779	6931.0775	6
			5	1	4	6665.8411	97.5	6931.0771		
			6	1	6	6622.4618	76.6	6931.0774		
5	2	3	5	1	4	6814.8663	89.5	7080.1023	7080.1023	1
			4	2	2	6858.2667	72.1	7080.1027		
			5	2	4	6786.4654	93.3	7080.1018		
			6	2	4	6676.5535	81.8	7080.1023		
5	2	4	4	1	3	6887.0126	95.9	7069.9960	7069.9962	6
			5	1	5	6844.1313	94.2	7069.9961		
			4	2	3	6852.9538	66.2	7069.9957		
			5	2	3	6766.0017	90.0	7069.9964		

TABLE 3—Continued

J'	Upper K'_a	K'_c	J	Lower K_a	K_c	Line position, in cm^{-1}	Transmit., in per cent	Upper energy, in cm^{-1}	Mean value, in cm^{-1}	δ in 10^{-4} cm^{-1}
	1			2		3	4	5	6	7
			6	2	5	6685.1210	77.7	7069.9963		
			5	3	3	6696.3310	97.1	7069.9967		
6	1	6	5	1	5	6785.8853	69.2	7011.7500	7011.7493	9
			5	0	5	6789.8026	98.1	7011.7486		
			6	1	5	6649.2428	97.7	7011.7496		
			7	1	7	6607.3042	80.2	7011.7496		
6	2	5	6	1	6	6853.2632	95.3	7161.8787	7161.8787	15
			5	2	4	6868.2429	70.0	7161.8793		
			6	2	4	6758.3296	94.4	7161.8784		
6	2	4	5	2	3	6875.2096	74.7	7179.2042	7179.2041	-13
			6	2	5	6794.3294	94.9	7179.2048		
			7	2	5	6659.0803	87.6	7179.2034		
7	1	7	6	1	6	6796.5116	69.7	7105.1272	7105.1260	-45
			7	1	6	6631.2102	98.4	7105.1275		
			8	1	8	6591.9175	80.3	7105.1244		
			8	1	7	6669.7934	97.5	7268.3561	7268.3548	-1
			7	3	5	6691.4520	98.2	7268.3563		
			6	2	5	6883.4779	69.1	7268.3533		
9	1	9	8	0	8	6813.1972	74.2	7325.7128	7325.7140	2
			8	1	8	6812.5065	97.6	7325.7135		
			10	0	10	6556.7868	80.9	7325.7165		
			10	1	10	6556.5958	95.4	7325.7122		
9	1	8	8	1	7	6889.5707	80.6	7488.1334	7488.1341	-1
			9	0	9	6853.7062	97.2	7488.1341		
			9	2	7	6686.4915	97.7	7488.1349		
			10	1	9	6603.0697	94.5	7488.1340		

And most differences between our upper energies and those from (12) are close to our experimental uncertainty.

(c) Different sets of ground state rotational energies were used as a basis for the ground state combination differences method in our analysis and in Ref. (12).

Upper energies obtained from the experimental transitions and presented in columns 2, 5, and 8 of Table 2 and in column 6 of Table 3 and Table 4 were used in the fit procedure with the Hamiltonian [1]–[5]. Results of the fit are presented in Table 5 and Table 6 together with 1σ statistical confidence intervals for the obtained parameters. The parameters of the states (101) and (210) which are presented without confidence intervals were fixed to the values of the corresponding parameters of the ground vibrational state from Ref. (15).

Comparing the corresponding parameters in different columns of Table 5, one can see that all values are suitable to the physics. In particular, the values of all rotational and centrifugal distortion parameters correlate both with each other and with the values of the corresponding parameters of the ground vibrational state (the latter are borrowed from Ref. (15) and presented in column 2 of Table 5), and vary more or less smoothly (with only two exceptions, namely, parameters Δ_{JK} for the states (021) and (210)) with the increase of the quantum number v_2 . As to the resonance interaction parameters, one can see in Table 6 that some types of resonance interactions appear in the fit besides the ordinary Fermi and Coriolis type interactions between the pairs of

states (101)/(021), (210)/(130), and (130)/(050). They are listed in Table 7. Columns 3 and 4 of that table show the type of terms in the effective Hamiltonian (I) which supplement the main resonance interaction parameters of the corresponding resonance operator and their order of magnitude in units of order of κ with respect to the order of the value of the rotational parameters (κ is the small Born–Oppenheimer parameter, (16), which in our case has a value on the order of 0.1). Column 5 presents the values of the corresponding resonance interaction parameters obtained from the fit. One can see a satisfactory agreement between the values of the parameters and the theoretically estimated orders of magnitude.

The reproductive power of the parameters obtained from the fit can be mentioned as one more confirmation of their correctness. To illustrate the correctness of the parameters, columns 4, 7, and 10 of Table 2 and column 7 of Table 3 and Table 4 present the values of differences $\delta = E^{exp} - E^{calc}$ in units of 10^{-4} cm^{-1} . One can see that in the overwhelming majority of cases the values of δ are close to the corresponding experimental uncertainties. The accuracy of reproduction decreases, of course, with increasing quantum numbers J and K_a because the strengths of the corresponding transitions decrease.

The statistical information on reproduction of the initial experimental energies with the parameters obtained from the fit also may be interesting: 304 energies (77.2% of all obtained upper energies) are reproduced with accuracy $|\delta| \leq 10 \times 10^{-4} \text{ cm}^{-1}$; 57 energies (14.5%) with accuracy $10 \times 10^{-4} \text{ cm}^{-1} < |\delta| \leq$

TABLE 4
List of Transitions Belonging to the $\nu_1 + 3\nu_2$ Band of HDO

J'	Upper K'_a	K'_c	J	Lower K_a	K_c	Line position, in cm^{-1}	Transmit., in per cent	Upper energy, in cm^{-1}	Mean value, in cm^{-1}	δ in 10^{-4}cm^{-1}
	1			2		3	4	5	6	7
3	0	3	2	0	2	6894.2049	92.5	6940.3780	6940.3786	-19
			2	1	2	6882.2522	94.8	6940.3791		
			3	1	2	6823.9170	88.4	6940.3782		
			4	0	4	6790.2222	96.0	6940.3783		
4	0	4	4	1	4	6783.9970	95.7	6940.3792	7000.5304	20
			3	1	3	6900.1398	97.8	7000.5306		
			5	2	3	6696.5360	89.4	7000.5307		
			3	2	1	6843.4654	85.3	7000.5301		
5	0	5	4	1	4	6912.6798	89.6	7069.0620	7069.0626	19
			4	0	4	6918.9069	92.3	7069.0630		
			5	2	4	6775.4270	95.5	7069.0634		
			6	2	4	6665.5138	97.2	7069.0626		
			5	3	2	6694.6529	99.2	7069.0627		
5	1	4	4	3	1	6829.9375	81.8	7125.6148	7125.6150	0
			5	3	3	6751.9493	87.0	7125.6150		
			6	3	3	6655.9518	87.9	7125.6151		
5	4	1	5	5	0	6774.6957	70.1	7390.6652	7390.6667	-48
			6	5	2	6681.4990	98.3	7390.6655		
			6	4	2	6816.6966	92.6	7390.6667		
5	4	2	5	5	1	6774.6957	70.1	7390.6651	7390.6667	32
			6	5	1	6681.4990	98.3	7390.6666		
			5	1	5	6927.4602	89.0	7153.3249		
6	0	6	5	0	5	6931.3797	93.4	7153.3257	7153.3256	-11
			6	2	5	6768.4503	97.7	7153.3256		
			5	2	3	6849.3322	95.7	7153.3269		
			9	4	5	6657.8625	90.9	7609.4970		
			9	3	7	6768.1278	92.7	7609.4945		
10	0	10	10	4	7	6503.2377	97.1	7609.5008	7609.4971	0
			11	4	7	6322.2624	98.1	7609.5000		
			9	4	5	6656.4251	91.8	7608.0596		
			10	4	7	6501.7956	13.6	7608.0587		
10	1	10	11	4	7	6320.8210	98.6	7608.0585	7608.0590	1

TABLE 5
Spectroscopic Parameters of the (101), (210), (021), (130) and (050) Vibrational States of the HDO Molecule (in cm^{-1})^a

Parameter	(000) ^b	(101)	(210)	(021)	(130)	(050)
1	2	3	4	5	6	7
E		6423.0693(249)	6753.146(142)	6444.7242(419)	6826.320(155)	6706.458(287)
A	23.413921	22.117353(466)	24.64489(131)	26.76440(203)	31.2430(219)	46.5026(107)
B	9.103359	8.915556(213)	8.874118(179)	9.374174(931)	9.31326(131)	9.73820(132)
C	6.4062805	6.228674(274)	5.910640(478)	6.34795(948)	6.054210(884)	6.01016(224)
$\Delta_K \times 10^2$	1.25878	1.08261(102)	2.6962(213)	3.74085(741)	8.756(140)	51.790(171)
$\Delta_{JK} \times 10^2$	0.11371	0.118557(818)	0.0472(115)	0.11928(894)	-0.0492(161)	-0.59280(925)
$\Delta_J \times 10^2$	0.036140	0.0350851(349)	0.036098(802)	0.051909(756)	0.07996(159)	0.076498(951)
$\delta_K \times 10^2$	0.21000	0.194491(703)	0.36925(281)	0.50373(238)	0.8840(446)	2.4098(232)
$\delta_J \times 10^2$	0.0121536	0.0122767(216)	0.014707(346)	0.014982(353)	0.030821(774)	0.025738(246)
$H_K \times 10^5$	4.9519	4.1287(344)	21.506(511)	31.790(344)	61.2612(867)	310.00(313)
$H_{KJ} \times 10^5$	-0.9269	-0.6278(241)	-0.9269	-3.6785(899)		
$H_{JK} \times 10^5$	0.2404	0.13989(605)	0.2404	1.2501(331)		0.939(114)
$H_J \times 10^5$	0.003996	0.003625(154)	0.003996	0.01336(102)	0.00836(221)	0.08985(589)
$h_K \times 10^5$	1.8366	1.2415(429)	2.666(212)	9.269(136)		
$h_{JK} \times 10^5$	0.1016	0.1016	0.1016	0.3858(153)		
$h_J \times 10^5$	0.002085	0.001278(101)	-0.000753(286)	0.00483(100)		
$L_K \times 10^7$	-2.5129	-1.8460(242)	-2.5129	-22.478(951)		
$L_{KKJ} \times 10^7$	0.8623	0.8623	0.8623			
$L_{KJ} \times 10^7$	-0.2408	-0.2408	-0.2408			
$L_{KJJ} \times 10^7$	-0.01062	-0.01062	-0.01062			
$l_K \times 10^7$	-1.9116	-1.9116	-1.9116			
$l_{JK} \times 10^7$	-0.00702	-0.00702	-0.00702			
$P_K \times 10^9$	0.5833			11.272(870)		

^a Values in parentheses are the 1σ statistical confidence intervals. Parameters presented without confidence intervals were fixed to the values of corresponding parameters of the ground vibrational state from Ref. (15).

^b Reproduced from Ref. (15).

TABLE 6
Parameters of Resonance Interactions between the States (101), (021), (210), (130), and (050)
of the HDO Molecule (in cm⁻¹)^a

Parameter	Value	Parameter	Value	Parameter	Value
Fermi Type Interactions					
$F_0^{101-021}$	14.8233(591)	$F_K^{101-021} 10$	-0.45169(289)	$F_J^{101-021} 10$	-0.171335(283)
$F_{KJ}^{101-021} 10^3$	-0.1215(189)				
$F_K^{021-210} 10$	-5.866(127)	$F_J^{021-210} 10$	-0.10935(869)	$F_{xyK}^{021-210} 10^3$	-0.8170(316)
$F_J^{021-130} 10$	-0.7431(584)	$F_{JJ}^{021-130} 10^3$	0.1974(254)	$F_{xy}^{021-130} 10$	-0.9457(220)
$F_{xyK}^{021-130} 10^3$	1.4507(529)				
$F_0^{210-130}$	28.48292(199)	$F_{KK}^{210-130} 10^3$	14.603(657)	$F_{JJ}^{210-130} 10^3$	-0.14647(543)
$F_{xyK}^{210-130} 10^3$	1.1130(621)				
$F_{xy}^{101-050} 10$	0.45188(983)	$F_{xyK}^{101-050} 10^3$	-1.2474(406)		
$F_0^{021-050}$	10.5471(109)	$F_K^{021-050} 10$	3.6926(550)	$F_J^{021-050} 10$	0.6288(213)
$F_K^{210-050} 10$	2.0993(471)	$F_{KK}^{210-050} 10^3$	9.461(473)	$F_{xyK}^{210-050} 10^3$	0.3588(565)
$F_{xyJ}^{210-050} 10^3$	0.03612(203)				
$F_0^{130-050}$	45.04887(312)	$F_K^{130-050} 10$	5.795(155)	$F_J^{130-050} 10$	-0.52724(430)
$F_{xy}^{130-050} 10$	0.28206(627)				
Coriolis Type Interactions					
$C_y^{101-021}$	0.161386(976)	$C_{yK}^{101-021} 10^2$	-0.4154(217)	$C_{yJ}^{101-021} 10^2$	0.08915(442)
$C_{zz}^{101-021} 10$	-0.001862(138)				
$C_y^{021-210}$	7.71231(464)	$C_{yK}^{021-210} 10^2$	3.6610(338)	$C_{yJ}^{021-210} 10^2$	0.5485(270)
$C_{yKK}^{021-210} 10^4$	-1.584(140)	$C_{yKJ}^{021-210} 10^4$	-0.2586(481)	$C_{zz}^{021-210} 10$	-3.1671(210)
$C_y^{021-130}$	1.70481(206)	$C_{yK}^{021-130} 10^2$	-4.261(194)	$C_{zz}^{021-130} 10$	-0.911(111)
$C_{zzJ}^{021-130} 10^4$	-8.223(567)				
$C_{zz}^{021-050} 10$	0.7721(189)				
$C_y^{130-050}$	0.7105(336)	$C_{yK}^{130-050} 10^2$	-2.432(233)	$C_{yJ}^{130-050} 10^2$	-0.6881(534)
$C_{zz}^{130-050} 10$	-0.5582(534)	$C_{zzK}^{130-050} 10$	-1.1173(320)		

^a Values in parentheses are the 1 σ statistical confidence intervals.

20×10^{-4} cm⁻¹; and 33 energies (8.3%) with accuracy 20×10^{-4} cm⁻¹ < $|\delta|$. In this case, if one takes into account that (a) HDO is a light molecule and (b) we fitted rovibrational energies of five vibrational states with high values of the quantum number v_2 for some of them, the total number of 117 fitted parameters looks not too large.

The question can be asked: why we did not used some other Hamiltonian model (i.e., the same Watson's type Hamiltonian, but with a Padé-type (17) summing up procedure) to reduce the number of fitted parameters? The answer can be in the following: the efficiency of Padé-type approximations strongly depends on the "quality" of initial experimental data which are used in a fit.

TABLE 7
Type of the Resonance Interactions Operators Which Were Taken into Account
in the Hamiltonian Model

Interacting states	Main type of interaction	Type of term	Order of magnitude	Value of param., in cm^{-1}
1	2	3	4	5
(021)/(210)	$C_y J_y$	$\langle qGJ_y \rangle \langle q^3 \rangle / \Delta E$	κ^2	3.856
(021)/(130)	$F_{xy}(J_x^2 - J_y^2)$	$\langle q^2 J_x^2 \rangle \langle q^3 \rangle / \Delta E$	κ^3	-0.095
(021)/(130)	$C_y J_y$	$\langle qGJ_y \rangle$	κ^1	0.852
(101)/(050)	$F_{xy}(J_x^2 - J_y^2)$	$\langle q^2 J_x^2 \rangle \langle q^3 \rangle / (\Delta E \Delta E')$	κ^3	0.024
(021)/(050)	F_0	$\langle q^4 \rangle$	κ^0	10.547
(021)/(050)	$C_{xz}(J_x J_z + J_z J_x)$	$\langle qJ_x J_z \rangle \langle q^3 \rangle / \Delta E$	κ^2	0.039
(210)/(050)	$F_K J_z^2$	$\langle q^2 J_z^2 \rangle \langle q^4 \rangle / \Delta E$	κ^4	0.210

For example, it is clear that Padé-type approximations (which, in principle, can be very efficient in the description of rovibrational energy structures of H_2O type molecules) have no advantages in comparison with the usual Watson Hamiltonian when initial experimental data do not contain states with high enough values of quantum numbers J and/or K_a . In accordance with the abovesaid, as our analysis shown, the using of Padé-type approximations in our present study will not reduce the number of fitted parameters. It can be affirmed that the relatively large number of fitted parameters in our study is the consequence of two reasons:

(a) It is, first of all, a complicated rovibrational structure caused by the presence of numerous different type accidental resonance interactions. In this case, the influence of irregular accidental resonances on the values of energy levels cannot be compensated for simply using some for Padé-type approximations or other.

(b) The second reason was our wish to achieve accuracies of theoretical reproduction of the initial experimental data which would be close to experimental uncertainties in the values of upper rovibrational energies. On the other hand, if one from such wish, the number of fitted parameters can be strongly reduced. For example, as the analysis shown, the mean reproduction of our experimental data with the accuracy of $0.002\text{--}0.003 \text{ cm}^{-1}$ can be achieved by the using of 55–60 fitted parameters only.

Comparison of the results of the present analysis with the results of the analogous high-resolution studies of the region near $1.4 \mu\text{m}$ (11, 12) may be interesting as well. The corresponding statistical information is presented in Table 8.

The paper, Ref. (18), should be mentioned here also. In that paper, parameters of the (210), (130), and (050) states and corresponding interaction coefficients are presented. Unfortunately, the total absence of any information in (18) both about assigned transitions, and upper energies obtained from

assigned transitions did not allow us to make correct comparison of our results and the results of Ref. (18). At the same time, we found that the upper energies of the (210), (130), and (050) states, being calculated with the parameters from

TABLE 8
Statistical Information Concerning Studied Bands
of the HDO Molecule

Value	Present study	Ref.(12)	Ref.(11)
$N_b^a)$	5	3	2
$n_{tr}^b)$	2070	1456	537
$J^{max}/K_a^{max}(101)$	16/8	15/8	13/7
$J^{max}/K_a^{max}(021)$	15/7	13/4 ^{c)}	11/7
$J^{max}/K_a^{max}(210)$	13/7	12/6 ^{c)}	-
$J^{max}/K_a^{max}(050)$	10/2	-	-
$J^{max}/K_a^{max}(130)$	10/4	-	-
$N_l^d)$	394	330	192
$n_p^e)$	117	-	38
m_1	77.2 ^{f)}	-	25.7 ^{g)}
m_2	14.5 ^{f)}	-	17.9 ^{g)}
m_3	8.3 ^{f)}	-	56.4 ^{g)}

^a N_b is the number of studied bands (without $2\nu_3$ band in Ref. (12)).

^b n_{tr} is the number of assigned transitions (without $2\nu_3$ band in Ref. (12)).

^c As was mentioned in the text, transitions with the upper values of quantum number $K_a = 5$ for the $2\nu_2 + \nu_3$ band and $K_a = 7$ for the $2\nu_1 + \nu_2$ band were misassigned in Ref. (12).

^d N_l is the number of obtained upper energies.

^e n_p is the number of fitted parameters.

^f Here $m_i = n_i/N_l \times 100\%$ ($i = 1, 2, 3$), and n_1, n_2 , and n_3 are the numbers of upper energies for which differences $\delta = E^{exp} - E^{calc}$ satisfy the conditions $\delta \leq 10 \times 10^{-4} \text{ cm}^{-1}$, $10 \times 10^{-4} \text{ cm}^{-1} < \delta \leq 20 \times 10^{-4} \text{ cm}^{-1}$, and $20 \times 10^{-4} \text{ cm}^{-1} < \delta$, respectively.

^g Since in Ref. (11) a theoretical reproduction of values of the upper energies is not mentioned, here $m_i = n_i/n_{tr} \times 100\%$; here the values n_1, n_2 , and n_3 have to do with the numbers of assigned transitions.

Ref. (18), reproduce our corresponding “experimentally” derived upper energies not “with mean accuracy of 0.003 cm^{-1} ,” as was proclaimed in (18), but with accuracy 30–100 times worse already for energy levels with the value of quantum number $J = 5, 6$ (in some cases, especially for rovibrational energies of the (050) state, differences can reach up to $1\text{--}2\text{ cm}^{-1}$).

5. CONCLUSION

The high-resolution Fourier transform spectrum of the HDO molecule was recorded and analyzed in the region of $6140\text{--}7040\text{ cm}^{-1}$ where the bands $\nu_1 + \nu_3$, $2\nu_2 + \nu_3$, and $2\nu_1 + \nu_2$, are located. Two thousand seventy transitions were assigned among which some tens were assigned to the transitions of the “dark” states $5\nu_2$ and $\nu_1 + 3\nu_2$. Strong local resonance interactions between all the “bright” and “dark” states were investigated and spectroscopic parameters of the analyzed bands were estimated. They reproduce initial upper energies with the accuracy close to the experimental uncertainties.

ACKNOWLEDGMENTS

This work was partially supported by the National Project for the Development of Key Fundamental Sciences in China, by the National Natural Science Foundation of China, by the Foundation of the Chinese Academy of Science, and by the Ministry of Education of Russian Federation. O. Ulenikov thanks the University of Science and Technology of China for a guest professorship, and E. Bekhtereva thanks the Ru Jia-xi Foundation for financial support during her stay in Hefei in March–May, 2001.

REFERENCES

1. Xiang-Huai Wang, O. N. Ulenikov, G. A. Onopenko, E. S. Bekhtereva, Sheng-Gui He, Shui-Ming Hu, Hai Lin, and Qing-Shi Zhu, *J. Mol. Spectrosc.* **200**, 25–33 (2000).
2. Sheng-Gui He, O. N. Ulenikov, G. A. Onopenko, E. S. Bekhtereva, Xiang-Huai Wang, Shui-Ming Hu, Hai Lin, and Qing-Shi Zhu, *J. Mol. Spectrosc.* **200**, 34–39 (2000).
3. Shui-Ming Hu, O. N. Ulenikov, G. A. Onopenko, E. S. Bekhtereva, Sheng-Gui He, Xiang-Huai Wang, Hai Lin, and Qing-Shi Zhu, *J. Mol. Spectrosc.* **203**, 228–234 (2000).
4. O. N. Ulenikov, Sheng-Gui He, G. A. Onopenko, E. S. Bekhtereva, Xiang-Huai Wang, Shui-Ming Hu, Hai Lin, and Qing-Shi Zhu, *J. Mol. Spectrosc.* **204**, 216–225 (2000).
5. Jing-Jing Zheng, O. N. Ulenikov, G. A. Onopenko, E. S. Bekhtereva, Sheng-Gui He, Xiang-Huai Wang, Shui-Ming Hu, Hai Lin, and Qing-Shi Zhu, *Mol. Phys.* **99**, 931–937 (2001).
6. A. Campargue, E. Bertseva, and O. Naumenko, *J. Mol. Spectrosc.* **204**, 94–105 (2000).
7. O. Naumenko and A. Campargue, *J. Mol. Spectrosc.* **199**, 59–72 (2000).
8. O. Naumenko and A. Campargue, E. Bertseva, and D. Schwenke, *J. Mol. Spectrosc.* **201**, 297–309 (2000).
9. H. Partridge and D. Schwenke, *J. Chem. Phys.* **106**, 4618–4639 (1997).
10. W. S. Benedict, N. Gailar, and E. K. Plyler, *J. Chem. Phys.* **24**, 1139–1165 (1956).
11. T. Ohshima and H. Sasada, *J. Mol. Spectrosc.* **136**, 250–263 (1989).
12. R. A. Toth, *J. Mol. Spectrosc.* **186**, 66–89 (1997).
13. Per Jensen, S. A. Tashkun, and V. I. G. Tyuterev, *J. Mol. Spectrosc.* **168**, 271–289 (1994).
14. J. K. G. Watson, *J. Chem. Phys.* **46**, 1935–1949 (1967).
15. N. Papineau, C. Camy-Peyret, J.-M. Flaud, and G. Guelachvili, *J. Mol. Spectrosc.* **92**, 451–468 (1982).
16. D. Papoušek and M. R. Aliev, “Molecular Vibrational–Rotational Spectra.” Elsevier, Amsterdam/Oxford/New York, 1982.
17. O. L. Polyansky, *J. Mol. Spectrosc.* **112**, 79–87 (1985).
18. A. D. Bykov, O. V. Naumenko, L. N. Sinita, B. P. Winnewisser, M. Winnewisser, P. S. Ormsby, and K. Narahari Rao, *Proc. SPIE Int. Soc. Opt. Eng.* **2205**, 248–252 (1993).